2004

Basic Study Of Micromachined Dep (dielectrophoretic) Manipulator

Vivek Sundaram
University of Central Florida

BASIC STUDY OF MICROMACHINED DEP (DIELECTROPHORETIC) MANIPULATOR

by

VIVEK SUNDARAM

B.E. Bharathidhasan University, 2000

A thesis submitted in partial fulfillment of the requirements
for the degree of Master of Science
in the Department of Electrical and Computer Engineering
in the College of Engineering and Computer Science
at the University of Central Florida
Orlando, Florida

Summer Term
2004

ABSTRACT

The capability of manipulating microparticle in small volumes is fundamental to many biological and medical applications, including separation and detection of cells. The development of microtools for effective sample handling and separation in such volumes is still a challenge. DEP (dielectrophoresis) is one of the most widely used methods in handling the microparticles. In this thesis we show that forces generated by nonuniform electric field (DEP) can be used for trapping and separating the microparticles (latex beads). This work further explores the DEP force based on different electrode geometries and medium conductivity. A micromanipulator for latex bead separation was designed, fabricated and characterized. For the development of DEP manipulator, the fabrication and packaging of microfluidic structure with the microelectrode is crucial for reliable analysis. A combination of SU-8 photoresist and polydimethylsiloxane polymer was used for this purpose. Besides, the DEP manipulator, preliminary study on a Coulter counter was conducted. The Coulter counter works on the principle of resistive pulse sensing. This counter is used for counting the beads as they pass through the microfluidic channel. Its possible integration with the manipulator was also explored.

ACKNOWLEDGEMENTS

Sincerest and heartfelt thanks to my advisor Dr.Hyoung J.Cho and Dr. K.B.Sundaram who have inspired, mentored, motivated and supported me through various educational, and personal triumphs and defeats. I am very thankful to Dr.Hyoung J.Cho for his careful reading of my thesis, helpful comments and inculcating the value of focused research in me. I also thank Dr.Hyoung J.Cho, Dr. K.B.Sundaram and Dr. Thomas X. Wu for agreeing to be on my thesis committee. I thank my friends, Hyungseok in achieving my task and for his useful suggestions; Shekhar for his empathy, insight and constant support and Anjum for his wonderful tips and goodness.

I am grateful to my great friends Rajeev, Sid, Sumant and Bhanu for their amazing company, their lively discussions, useful straightforward criticisms, for always being there for a shoulder to cry on and an ear to listen. My thanks to Rachel for being such a good friend.

Finally, I reserve my highest gratitude to my parents, brother and sister. Without the love, support and encouragement of my family I wouldn't be where I am today. This thesis is dedicated to my parents, to whom I am forever indebted.

TABLE OF CONTENTS

LIST OF FIGURES

CHAPTER 1. INTRODUCTION

... objects nonviewable to human watchers save 'twere perchance anon some glistery gleam darkling adown surface of affluvial flowandflow... - from James Joyce's Finnegans Wake

Detection of microorganisms such as bacteria is extremely important in a variety of fields especially in medical diagnosis and hazard analysis in food industry. Though using conventional microbiological detection methods such as a colony counting technique, based on cell incubation are sound and reliable but they are quite time consuming, requiring lot of time (few days) and thus are not capable of fast diagnosis in case of emergency [1]. In microorganism inspection and identification, there are many cases in which a specific bacterium is to be detected according to the species or its physiological state. This has led researchers to find ways and means for handling and detection of microorganisms in a much faster way. One such means is by manipulating micron and sub-micron sized particles.

1.1 Related Research

1.1.1 Particle Manipulation and Separation

The ability to manipulate particles, especially living cells, in three-dimensional space is fundamental to many biological and medical applications, including isolation and detection of sparse cancer cells, concentration of cells from dilute suspensions, separation of cells according to specific properties, and trapping and positioning of individual cells for characterization [1], [2]. Some of the physical forces that can be employed for particle

manipulation, including those of mechanical, hydrodynamic, ultrasonic, optical, and electromagnetic origin. These forces have been successfully employed for biological applications like cell sorting and characterization with flow cytometry [3], cell manipulation with laser tweezers [4], and cell separation with antibody-labeled magnetic beads [5]. Studies have also been reported on the electrical characterization of single cells in microstructures. They primarily use electronic properties of cells for concentration, transport and separation.

Intense research is going on in cell separation techniques due to its far reaching implications in numerous areas such as clinical medicine, detection of pathogenic organisms, cancer research and basic biological and materials research. Some of the cell separation techniques currently being used in biological laboratories, including isocypnic centrifugation that exploits cell density properties, and fluorescent or magnetic activated cell sorting that exploits cell immunological or receptor targets. Conventional fluorescence-activated cell sorters (FACS) are widely used to study eukaryotic cell populations. Although they provide impressively efficient cell sorting, they are very expensive and mechanically complex. In addition they are not user friendly and require trained personnel for operation and maintenance. Another difficulty occurs during high-speed FACS. Since higher pressures are required to achieve a rapid rate, limitations such as cell type and viability must be considered [6]. Conventional FACS suffers from the discrepancy between tool and object size. This mismatch hinders their integration with miniaturized, high-performance analytical systems. This necessitates fabrication of inexpensive devices. Devices that rapidly sort live cell, particles and even single molecules would greatly facilitate screening of combinatorial chemistry libraries or cell populations during in vitro molecular evolution.

1.1.2 BioChip

In recent years micro technology has developed at an astonishing rate. It has become an area where lots of researchers are focusing their vision. Miniaturization promises to do for biomedical testing what it did for electronics (integrated circuit): creating new technology, saving time and slashing costs. This has lead to a new concept of Lab-on-a-chip which as the name itself suggests stands for laboratories on a chip. This biochip is expected to have the same specialized functions as their room-sized counterparts. These chips can perform clinical diagnoses, scan DNA, run electrophoretic separations, act as microreactors synthesizing novel compounds, and are self-contained chromatographs.

The typical biochip is a thin glass or a plastic plate, a few centimeters on a side, with a network of microchannels etched on its surface. These microchannels are and can be few centimeters in length. The position of electrode plays a very important role in optimum operation of the device so they are placed at strategic locations on the chip. Usually, microfluidic channels and electrode form the basic infrastructure of the chip. A simple experiment is initiated by injecting a liquid sample (as little as several picoliters) at one end of the microchannel. The injection of the liquid is done at a predefined rate depending upon the experiment. Electric fields are generated through the electrodes. On such a chip, hundreds of such reactions can be performed simultaneously through numerous parallel microchannels. Thus the obtained information can be analyzed at the same time. The advantages of these biochips include very small consumption of sample, small size, very short reaction and analysis time and high throughput. Life sciences and diagnostics have greatly benefited from

the utilization of micro technology. Despite having numerous advantages, not many of these ideas have been realized.

Starting from the vision of a biochip, micro fluidic systems have created new opportunities for handling and analysis of small objects such as cells, beads or even molecules [7]. Precise manipulation of biological fluids is key to the performance of a bio chip. In order to operate, such a biochip device must be able to perform a sequence of chemical and biochemical reactions for analysis or synthesis. These integrated microsystems, whose basic infrastructure consists of electrical, mechanical and fluidic components have wide applications in biomedical research, clinical diagnosis, detection of food pathogen and environmental monitoring. For example, a microfluidic system can be used in the molecular analysis of cancer cells within a small volume of pathologic fluid to provide cancer prognostic information. A very critical necessity while using microsystems to process cell samples is that they should be able to discriminate and sort cells according to their characteristic phenotypes [8]. Although, cell separating techniques are very useful and very powerful in the macroscopic world, these techniques do not readily scale to microsystem applications. A physical-force mechanism which is dependent on the properties of cell and effective on the microscopic scale is therefore desirable. One such mechanism is dielectrophoresis (DEP). It is generated by the microelectrodes and requires no mechanical contact with cells and is an effective mechanism for manipulating cells in microstructures. Early studies of cell dielectrophoretic responses employed electrode structures made from thin electrical wires, including cone-plate electrodes in a levitation system using conventional dielectrophoresis (cDEP); simple pin-plate structures [9].

1.2 Objective and Goals

This work will focus on sorting and counting of beads by two different phenomena of dielectrophoresis and Coulter counter. Sorting of the beads will be done using the translational motion of neutral matter caused by polarization effects in a nonuniform electric field known as *Dielectrophoresis.* It is to be carefully distinguished from motion caused by the response to free charge on a body in an electric field (uniform or non-uniform). The latter phenomenon is known as *electrophoresis*. And the counting of beads will be carried out using the *Coulter Principle*. Finally, we will try to integrate both DEP and Coulter counter on a single biochip.

CHAPTER 2. THEORY- DIELECTROPHORESIS AND COULTER COUNTER

The behavior of matter in electrical fields, especially nonuniform electric fields, is of interest to scientists of various branches: physics, chemistry, engineering or life sciences. To chemists and physicists it is a science of many and varied phenomena. To engineers it is a source of new and useful techniques for separating materials or improving materials behavior. To ecologists it provides a major means of minimizing pollution. To life scientists it offers new ways to study and manipulate cells and their sub-particles, and to help unravel the nature of living systems. It constitutes a novel method of separating and distinguishing cells that differ in kind or physiological state. The first separation of living from dead cells by purely physical means was accomplished using nonuniform field effects in 1966 by Pohl et al [9].

2.1 Dielectrophoresis

The two major electrokinetic techniques which have been applied to materials separation are electrophoresis and dielectrophoresis. The former technique involves the migration of charged matter under the influence of a uniform, steady electric field. Therefore, it is used to separate materials which already carry a charge or made to do so in a controlled manner and for this reason finds applications primarily in the separation of biological materials based on charge and/or size. Dielectrophoresis on the other hand, is the translational motion of neutral matter caused by polarization effects in a nonuniform (steady or oscillating) electric field. The electrical force on any object undergoing dielectrophoresis

is directly related to its volume and polarizability, which is a function of its complex permittivity, for a given medium and electric field [10].

Dielectrophoresis has a relatively simple physical origin. Any electric field, uniform or non-uniform, exerts a force upon a charged body. It is characteristic of non-uniform fields, however, that they exert a force upon neutral bodies. A wide variety of interesting and useful events take place as a result.

In a uniform electric field, a charged particle is pulled along the field lines towards the electrolyte carrying the charge opposite to that on the particle. But in the same electric field a neutral will just be polarized. The result might produce a torque, but not a net translational force. Thus the body as a whole will not move toward either electrode. In case, the body is anisotropically polarized, or if it is elongated, a torque can arise. The resultant dipole tends to align itself in the field. If the particle is isotropic and spherically symmetric, there would not be any torque as shown in figure 2.1.

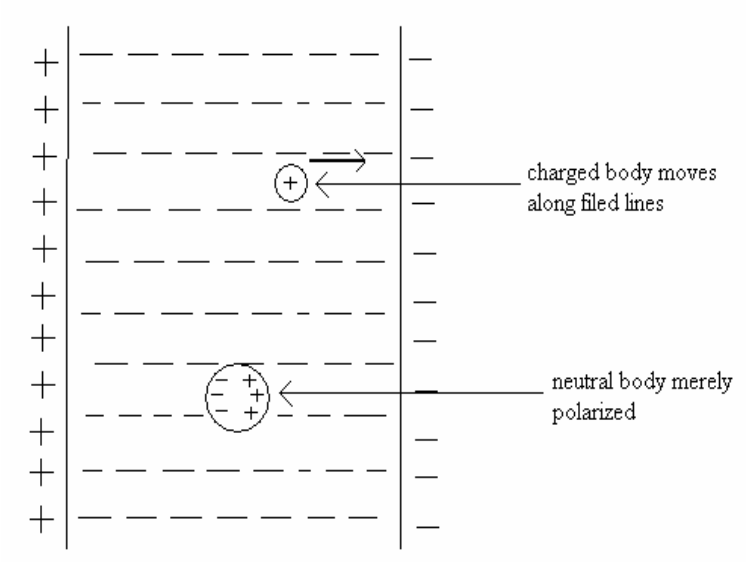

Figure 2.1 Comparison of behaviors of neutral and charged bodies in a uniform electric field

But in a nonuniform electric field, we see different behavior of the charged and uncharged objects. The charged one behaves much as before, being pulled along the field lines. It is still attracted toward the electrode of opposite polarity. But the neutral particle will in this case find a translational force upon it. The reason being that under the non-uniform electric field it gets polarized, putting a positive charge on the side nearer the negative electrode and vice-versa. Since the particle is neutral, the two charges on the body cancel out each other. The usual result of such a polarization of a neutral body in nonuniform field is to bring about an impelling in the neutral body toward the region of stronger field. Inhomogeneous, high frequency a.c. electric fields can be used to manipulate molecules and particles by dielectrophoresis. Positive dielectrophoresis (p DEP) is the movement of a dielectric toward regions of high field strength; it can cause damage as particles are attracted to the electrodes.

Less stress is induced, especially in living cells, when the particles move toward field minima (negative DEP) as shown in figure 2.2. Movement of the particles depends on driving frequency and on the dielectric properties of particles and surrounding liquid. Dielectrophoresis has been applied to separating a variety of materials. Pohl and Schwar [1] demonstrated the separations of organic and inorganic powders in and from liquid dielectrics [9]. The yield was found, in agreement with theory, to depend on a variety of factors such as field strength and gradient, particle size etc. With further modifications to this apparatus, it was also possible to utilize this technique to allow continuous separations [3]. In this case, however, it was noted that the obtained efficiency of the separations actually exceeded the theoretically expected values.

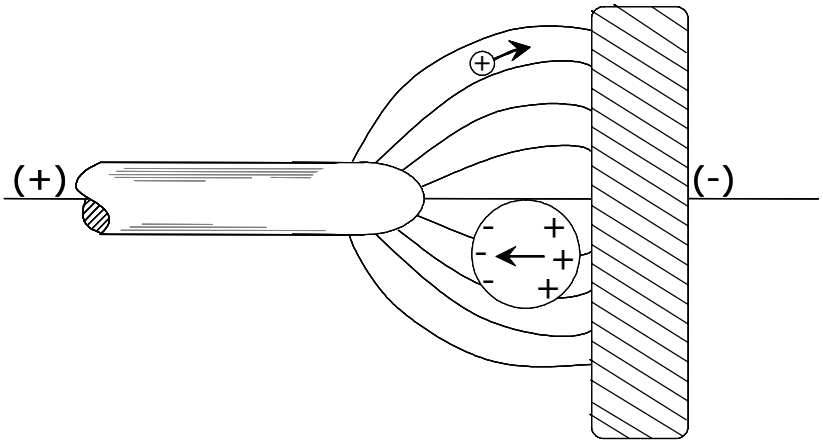

(a)

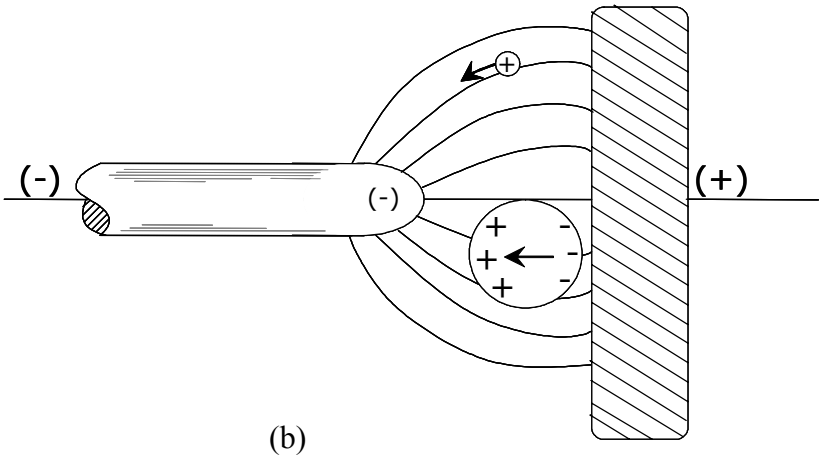

(b)

Figure 2.2 The influence of an electric field on a microparticle (a) In medium of low conductivity the bead is being polarized and moves towards areas of higher electric field, towards the anode. (b) In media of high conductivity positive charges accumulate opposite the anode and the cell is subjected to negative dielectrophoresis and thus is being repelled from the electrodes.

We can compare dielectrophoresis and electrophoresis as follows**:**

1) Dielectrophoresis produces motion of bodies suspended in a fluid medium. The direction of the motion is independent of the polarity of the field. Accordingly, either a.c. or d.c. fields can be used. Electrophoresis produces a motion of the suspended particle in which the direction of the resultant path depends upon both the polarity of the charge on the particle and upon the polarity of the field direction. Reversal of the field reverses the direction of travel. But on certain occasion the motion of the charged particles can be towards a sharp electrode if an a.c. field of high strength is present. This occurs because of space charge effects and the appearance of partial rectification or selective charge injection.
2) Dielectrophoresis gives rise to an effect which is proportional to the particle volume and is therefore more easily observed on coarse particles. Electrophoresis is observable with particles of any size; atomic ions, molecular ions, charged colloidal particles, or charged macroscopic bodies.
3) Dielectrophoresis usually requires quite divergent fields for strong effects. Electrophoresis operates both in uniform and divergent fields.
4) Dielectrophoresis requires relatively high field strengths. With previously charged particles (e.g. ions, charged sols), electrophoresis requires relatively low fields. Strong fields may cause space-charging in the fluid (gas or liquid) dielectric, with subsequent deposition of charges upon previously neutral particles, and a resultant electrophoretic force.

5) Dielectrophoresis usually requires a substantial difference in the relative permittivities of the particle and the surrounding medium. Electrophoresis can be appreciable even when the free charge per unit weight of the particle is quite small.

2.1.1 Bunching Effect and Pearl-Chain Effect

Clumping or bunching of a group of neutral particles caused by an applied electric field is known as bunching effect [9]. It is particularly evident when particles of high dielectric constant suspended in a medium of lower dielectric constant are subjected to an external electric field and undergo dielectrophoresis. Particles undergoing dielectrophoresis often exhibit a mutual attraction. Suspended particles are observed to clump or bunch together even in uniform electric field. This is *mutual dielectrophoresis*, and arises in the following way. The particles which have polarizability larger than that of the surrounding medium, distort the field. Each particle then experiences a nonuniform field near each other. As they are already polarized by the external field, the particles are then attracted to the regions of higher field intensity. The bunching effect due to the enhancement of field nonuniformity by the particles themselves frequently causes the formation of 'pearl chains' or other clusters in an electric field. The association of suspended particles by the bunching effect frequently increases the rate at which particles in concentrated suspensions are removed by the action of nonuniform field effects, because of the reduced viscous drag on the aligned particle assembly.

2.1.2 Average Position of a Charged Particle in a NonUniform Electric Field

In the case of a charged particle situated in an a.c. but uniform field (as between parallel-plate electrodes), the time-average position of the particle will be unchanged. In the case of a charged particle in a nonuniform a.c. field, it is not quite so evident that the position should remain constant on average. Let us consider a spherical particle of charge q, radius a and mass m, in a fluid of viscosity η. Let it be subject to an a.c. field,

$$E = E_0 e^{i\omega t}$$

where

ω is the angular frequency

E_0 is the maximum amplitude of the field

Neglecting dielectrophoretic forces for the time being, the total instantaneous forces on the particle will then be [9]

$$F_i + F_\eta + F_C = 0$$

where

F_i = -mr = inertial restraint

F_η = -6Παηr = Stokes' drag or viscous force (Π = 22/7)

F_C = qE = Coulombic force

To particularize, let us calculate the case for a spherical particle sitting in a cylindrically symmetric field where r is the radial coordinate and $\hat{r}$ is the unit vector. Then

$$E = E_0 \hat{r} / r$$

and the equation of motion is [9]

$$mr + 6\pi a \eta r - \frac{qE_0 \hat{r_0} e^{i\omega t}}{r} = 0$$

The approximate solution can be found (neglecting the small inertial force due to low field limit) by integrating,

$$6\pi a \eta r dr = qE_0 \hat{r_0} e^{i\omega t} dt$$

hence,

$$6\pi a \eta \int_{r_1}^{r} r dr = qE\hat{r_0} \int_{0}^{t} e^{i\omega t} dt$$

$$3\pi a \eta \left[r^2 - r_1^2 \right] = \frac{qE\hat{r_0}}{i\omega} \left[e^{i\omega t} - 1 \right]$$

For "n"full cycles,

$$t = n/\nu = 2\pi \frac{n}{\omega}$$

But since $e^{i2\pi n} = 1$, where n = 0, 1, 2… integer, then

$\left\langle r^2 \right\rangle_{fc} = r_1^2$ or $\left\langle r \right\rangle = r_1$ = constant

where $\left\langle r^2 \right\rangle_{fc}$ means the full cycle of mean r^2.

2.1.3 Microelectrodes

Recent advancement in microfabrication technology has enabled the production of number of microelectrode arrays suitable for particle manipulation. Examples include polynomial electrode arrays for cell separation by trapping cells of different types at different locations using positive and negative cDEP forces [11], various three-dimensional microelectrode arrays for cell positioning, trapping and levitation [12], [13],[14].

To study real electrode arrangements, the electric field has to be calculated numerically [7]. Finite different method is used for the complex electric field

$$\vec{E}(\vec{r},t) = \mathrm{Re}[(\vec{E}^{re}(\vec{r}) + i\vec{E}^{im}(\vec{r}))\exp(i\omega t)] \tag{1}$$

where ω is the radian frequency.

The time-averaged dielectrophoretic force acting on a particle of radius R can be calculated in dipole approximation for known electric field distribution $\vec{E}(t)$ as:

$$\begin{aligned} <\vec{F}_{DEP}> = 2\Pi\varepsilon_1 R^3 \times [&\mathrm{Re}(f_{CM})\vec{\nabla}\sum_{\mu}\{(E_{\mu}^{im})^2 + (E_{\mu}^{im})^2\} \\ &+ \mathrm{Im}(f_{CM})\sum_{\mu,v}\{(E_{\mu}^{re}\frac{\partial E_{\mu}^{im}}{\partial v} - E_{\mu}^{im}\frac{\partial E_{\mu}^{re}}{\partial v})\vec{e}\}] \end{aligned} \tag{2}$$

The Clausius-Mosotti factor, $f_{CM,}$ reflecting the dielectric properties (permittivity ξ and conductivity σ) of particle (index p) and surrounding liquid (index l), becomes, for a homogenous sphere,

$$f_{CM} = \frac{\tilde{\varepsilon}_p - \tilde{\varepsilon}_l}{\tilde{\varepsilon}_p + 2\tilde{\varepsilon}_l} \qquad (3)$$

with the complex permittivity $\tilde{\varepsilon} = \sigma + i\omega\varepsilon_0\varepsilon$

The first term in equation (2) is proportional to the gradient of the mean square value of the electric field strength; the second one is proportional to the gradient of the field phase. Hence we deduct that individual manipulation of single particles requires field inhomogeneities with dimensions similar to those of the particles. For the a.c. case, without gradient in the phase, the conditions for negative dielectrophoresis are fulfilled for

$$\text{Re}\,(f_{CM}) < 0 \qquad (4)$$

i.e. if the absolute value of the complex permittivity of the particle is lower than that of the suspending liquid. Due to the high permittivity of water, polymer particles and living cells exhibit negative dielectrophoresis at high-field frequencies.

2.2 Coulter Counter

Coulter's principle of volumetric impedance calls upon the principle of displacement as a measure of volume [16], [17]. The underlying idea of the principle is based upon resistive pulse sensing. It is a method by which presence of a particle is detected by sensing the change in resistance along a liquid filled capillary due to the flow of particle. For example, blood cells are suspended in a conductive fluid into which electrodes are placed. As a blood cell passes through an aperture between the electrodes, it displaces its own volume of electrolyte. This displaced volume causes change in resistivity measured in the electrolyte from one side of the aperture to the other. As a result we get a resistance spike across the two electrodes. The signal which is recorded due to change is resistivity implies a transient signal

for each passing cell. From the recorded signal, we can count the number of cells and from the height and area of the pulses we can determine the size of the individual cells. Typical Coulter counter aperture ranges approximately between 30μm to 200μm [18]. Smaller the aperture higher the sensitivity of the Coulter counter. But the drawback is that smaller aperture leads to clogging [19]. Therefore there's always a trade-off between sensitivity and clogging. It is also important that the cells suspended in the fluid have lower conductivity than the fluid. Figure 2.3 illustrates a Coulter counter.

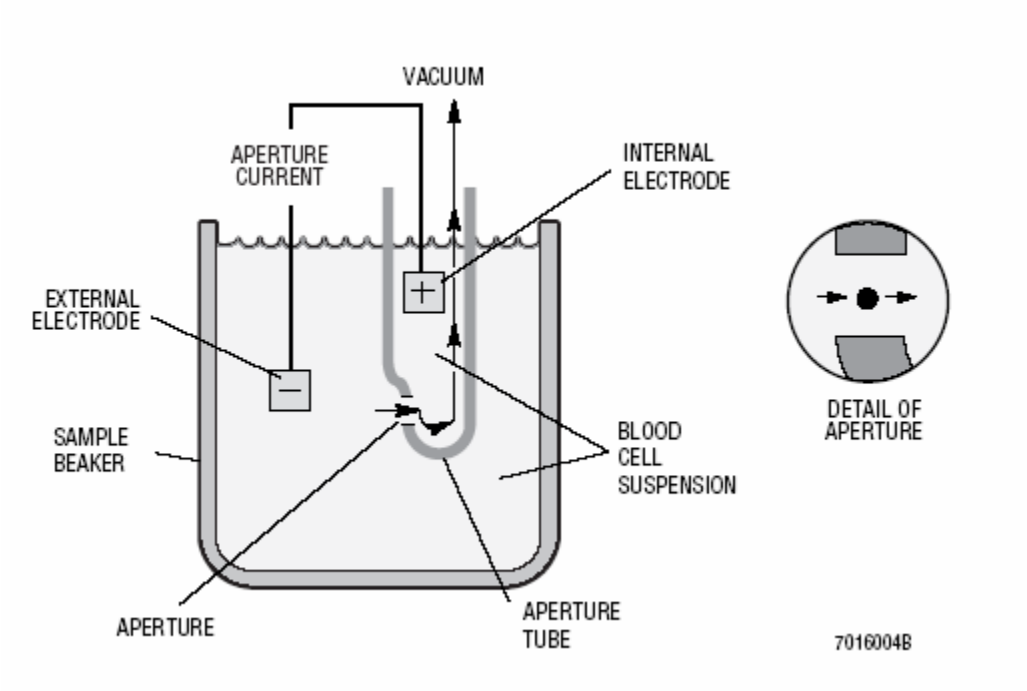

Figure 2.3 A typical Coulter counter

(http://www.beckman.com/products/instrument/partChar/pc_multisizer3.asp)

The conductivity of a solution depends on the number and type of ions present and thus on the molar concentration "c" [20]. The molar conductivity is defined as:

$$\Lambda_m = \kappa / c$$

where

Λ_m = molar conductivity

κ = conductivity of the fluid

c = molar concentration

The measured resistance in a channel with electrolyte depends both upon the conductivity and the geometry. If the cross-sectional area is constant, the resistance is given by:

$$R = 1/ (c. \Lambda_{m)} . l / A$$

where

R = resistance of the electrolyte

l = length of the cross-sectional area of the channel being observed

a = cross-sectional area of the channel being observed

2.3 Micromachining

Traditionally, X-ray lithography has been a major technique for fabricating ultra-thick microstructures with millimeter-sized thickness. Microstructures with very high aspect-ratio, vertical sidewalls and high resolution have been reported using the LIGA (lithographic, galvanoformung und abformung) technique [29]. However, the exorbitant cost of synchrotron radiation source and the time consuming process limits its application for researchers. The fabrication of high-aspect-ratio microstructures by standard UV lithography has been popularized by the advent of EPON SU-8 epoxy-resin negative photoresist.

The SU-8 is a negative, epoxy-type, near –UV, PR based on the EPON SU-8 resin. It can be obtained by dissolving the EPON resin SU-8 in the organic solvent GBL (gamma-butyiloractone). The quantity of the solvent determines the viscosity and thereby the thickness ranges of the resist. Finally a photointiator is added: 10 wt% of the resin mass.

Since it is a thick, epoxy-photoplastic, high aspect ratio resist, it finds application in several MEMS areas, including the fabrication of plastic micromolds or metal micromolds by electroplating [30]. Being a UV sensitive resist it can be spin coated in a conventional spinner in thicknesses ranging from 1μm to 300μm, while up to 2mm thicknesses can be obtained by multilayer coatings. Combined with standard lithographic processes, SU-8 offers excellent opportunities in MEMS application and packaging. SU-8 has the following advantages: (i) once polymerized it has excellent mechanical and chemical properties, (ii) it enables the formation of deep trenches and extremely rigid structures by standard UV photolithographical means, (iii) it is a relatively inexpensive technology for high aspect ratio feature formation compared to other techniques, e.g. LIGA or dry etching techniques, (iv) its is a compatible material for analysis by mass spectrometry. Fabrication procedures for a typical SU-8 photoresist is illustrated in figure 2.4.

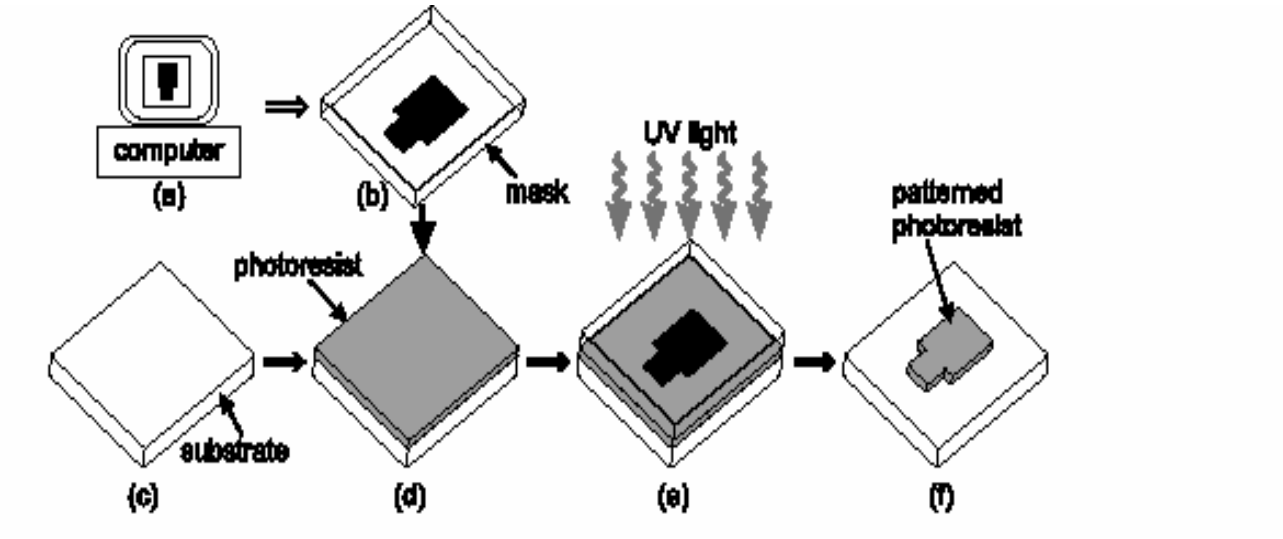

Figure 2.4 Fabrication steps of a SU-8 photoresist [21]

SU-8 has very suitable properties of thickness and chemical stability, and has some good mechanical and optical properties as well. However, despite all these advantages, the SU-8 photoresist suffers from three disadvantages, namely adhesion selectivity, stress and resist stripping. Some critical properties that need to be controlled are listed.

Adhesion selectivity

SU-8 adhesion is good on materials such as silicon and gold [31], but on other materials such as glass, nitrides, oxides and other metals, the adhesion is poor and the resist easily delaminates from such material surfaces during development. Adhesion can be improved on certain surfaces by using a suitable adhesion promoter, or by using additives to the SU-8.

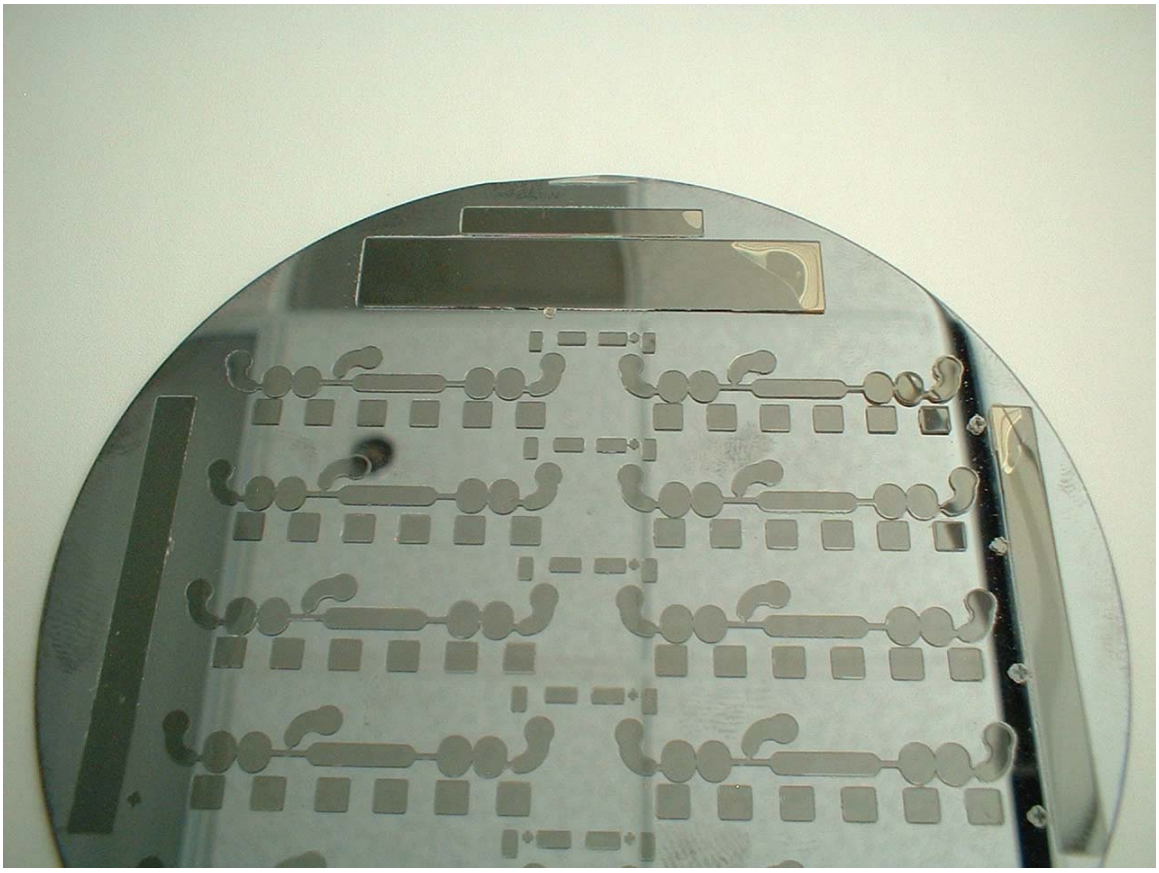

Figure 2.5 A typical silicon wafer on which microchannels have been fabricated using SU-8

Stress

On many suitable surfaces for spinning SU-8 such as silicon or glass, the thermal expansion coefficient mismatch is large (SU-8 has a thermal expansion coefficient of 52ppm K^{-1} compared to silicon which has a coefficient of 3ppm K^{-1}). This causes large amounts of stress material interface due to shrinkage of the resist while cross-linking during curing. This stress effect is pronounced in large SU-8 structures, and if poor adhesion is obtained during processing, the photoresist delaminates easily. Low thermal expansion coefficient can somewhat alleviate this problem.

Resist stripping

As a photoplastic material, SU-8 is chemically stable and resistant to most acids and other solvents. Consequently, it is difficult to remove once cross-linked and suitable methods of stripping are often not effective or desirable to use. However, these three disadvantages lend themselves well to certain MEMS applications where it is not desired to remove resist. Small, and hence low-stress, SU-8 structures patterned with good adhesion on silicon can be used as functional or permanent material when combined with conventional MEMS processes and materials.

The challenges for fabricating an ultra-thick microstructure include PR coating, baking process, PR developing efficiency and tremendous residual stress formed after the curing of SU-8. Microstructure with a height of 1.2mm has been reported [32] by double-coating the SU-8 PR layers [32]. However, multi-coating is a time consuming process. The surface flatness is also a critical issue. The solvent content in subsequent coating layers may be different, resulting in a much more complicated lithography process. Also single coating of an SU-8 film thicker than 1mm is not practical using a conventional spin coater [29]. Besides at low speed, the high viscosity of the SU-8 will lead to a poor PR coverage.

Another problem caused by spin coating is the *'edge-bead effect'*, which occurs for films thicker than 50μm [30]. During the soft-baking the re-flow of the PR also changes the thickness of the coated films. The problem becomes more serious when thicker PR layers are coated using substrates with irregular shapes. The existence of the edge-bead will cause photomasks not be completely in contact with the PR. Consequently, this will cause a bad lithography image due to the air gap between the photomasks and the substrates. One possible solution for this problem is to remove the edge-bead by standard edge-bead removal

techniques with γ -butyrolactone (GBL). Alternatively, one can fill the air gap with organic solvents. However, the organic solvent will form a slippery layer and it may diffuse into the SU-8 layer, forming a fragile structure.

The baking process is another important issue for the fabrication of ultra-thick SU-8 microstructures. In previous works based on the Taguchi method, it has been reported that the soft-baking conditions of a thick SU-8 film are very critical for its lithographic quality [30], [33], [34] and it has been indicated that an improper post-exposure bake (PEB) procedure tends to distort fine-line features [30]. Normally, it takes tens of hours to bake an SU-8 film thicker than 1mm at a standard baking temperature of 95^0C.

Another problem commonly encountered during the lithography process is the distortion of the microstructures. The thermal expansion coefficient (TEC) of SU-8 is 52 ± 5.1ppm $^0C^{-1}$ [36]. It has been noticed that unexposed SU-8 might be squeezed out of a channel due to the thermal expansion of the exposed region, resulting in a distorted geometry. The problem caused by thermal expansion becomes more serious when the exposed area is bigger. Likewise; large internal stress for the polymerized SU-8 is a big problem for the fabrication of ultra-thick microstructures. Not only does internal stress distort the patterned structures but it also causes some adhesion problems or even cracking failures [32] and [35]. Detailed information regarding the quantity measurement of the stress induced by the polymerization of SU-8 has been reported in the literatures [32], [37],[38]. The effect caused by the large internal stress can be alleviated either by reducing the exposed area or by generating a discrete small-sized exposed region.

2.4 Microfluidics

Microfluidics is a traffic control system for sampling, sorting, and mixing mesoscopic objects. The objects are often biological-cells, proteins, chromosomes in a solvent-and the platform is often a lithographically patterned chip on which fluids are infused through microchannels using volts, heat, or even peristaltic pressure.

In recent times, the development of micro-fluidic systems based on MEMS technologies has been attracting significant scientific and industrial attention. Microfluidic devices have been described for many applications e.g. chromatography, bioanalysis, capillary electrophoresis etc. Many applications of microfluidic devices are compatible with, or require, large channels (>200μm), and it must be possible to connect them easily to the outside world.

Rapid prototyping of microfluidic devices is important in a research setting where it is necessary to complete multiple cycles of design, fabrication, and testing in a short period of time. The two most commonly used materials are silicon or glass. Use of these materials and techniques, such as reactive ion etching (RIE) and fusion bonding for developing micro-fluidic devices has not only resulted in high cost, but also many limitations on fabrication, packaging and testing.

Many plastic materials have been investigated as candidate massive replication materials for MEMS. Examples include polycarbonate (PC) [21], polymethyl methacrylate (PMMA) [22], polyvinyl chloride (PVC), polyethylene (PE) [23], and polydimethylsiloxane (PDMS) [24].

PDMS replication has been utilized mostly in microfluidics with the use of epoxy-based photoresist SU-8 as mold inserts. A fluidic switch and a side channel flow controller have been fabricated in PDMS against SU-8 master for micro total analysis systems (μTAS) [39]. Three-dimensional micro-channels in PDMS with a sandwich-molding configuration have been developed for complex 3-D channel paths [40].

Polydimethylsiloxane (PDMS) is a microelectronics compatible type of silicone elastomer [41]. PDMS is durable, optically transparent, and inexpensive. PDMS has a low glass transition temperature (T_g » -125°C) and can be used over a wide temperature range (approximately from –100°C to 100°C). It is very flexible (a shear modulus between 100 KPa and 3MPa) and highly compressible without mechanical failure [42]. It also has high dielectric strength (~ 14V/mm). Chemically, it is non-toxic, very stable due to its low reactivity, and possesses high gas permeability. It is commercially available from many manufacturers (Sylgard 184, Dow Corning, Midland, MI). PDMS replication has been utilized mostly in microTAS applications and processed with patterned SU-8 as mold inserts [43].

The use of microfluidic devices to conduct biomedical research and create clinically useful technologies has a number of significant advantages. First, because the volume of fluids within these channels is very small, usually several nanoliters, the amount of reagents and analytes used is quite small. This is especially significant for expensive reagents. The fabrications techniques used to construct microfluidic devices are relatively inexpensive and are very amenable both to highly elaborate, multiplexed devices and also to mass production. In a manner similar to that for microelectronics, microfluidic technologies enable the fabrication of highly integrated devices for performing several different functions on the

same substrate chip. One of the long term goals in the field of microfluidics is to create integrated, portable clinical diagnostic devices for home and bedside use, thereby eliminating time consuming laboratory analysis procedures.

CHAPTER 3. DESIGN AND FABRICATION

The DEP manipulator and the Coulter counter consist of two layers. The bottom layer has the electrode. The top layer is made up of PDMS layer, which has the microfluidic channels. These channels are obtained by casting a mixture of prepolymer PDMS and curing agent on the SU-8 microstructures. Finally, the whole device is assembled by covering the PDMS layer with an acrylic lid so as to ensure uniform pressure and to hold the device strongly.

3.1 DEP Electrode

3.1.1 Design

Electrode design was investigated for DEP sensor. The electrode layer consists of different electrode geometries.

The basic principle of DEP underlines that a nonuniform a.c. electrical field has to be generated to create DEP force. Accordingly, the most important design considerations are electrode geometry and electrode dimensions. Electrode design was carried out using AutoCAD software. Design was then transferred on a mask. A number of electrodes with different electrode geometries and dimensional variations were designed as shown in figure 3.1.

3.1.2 Geometry and Dimension

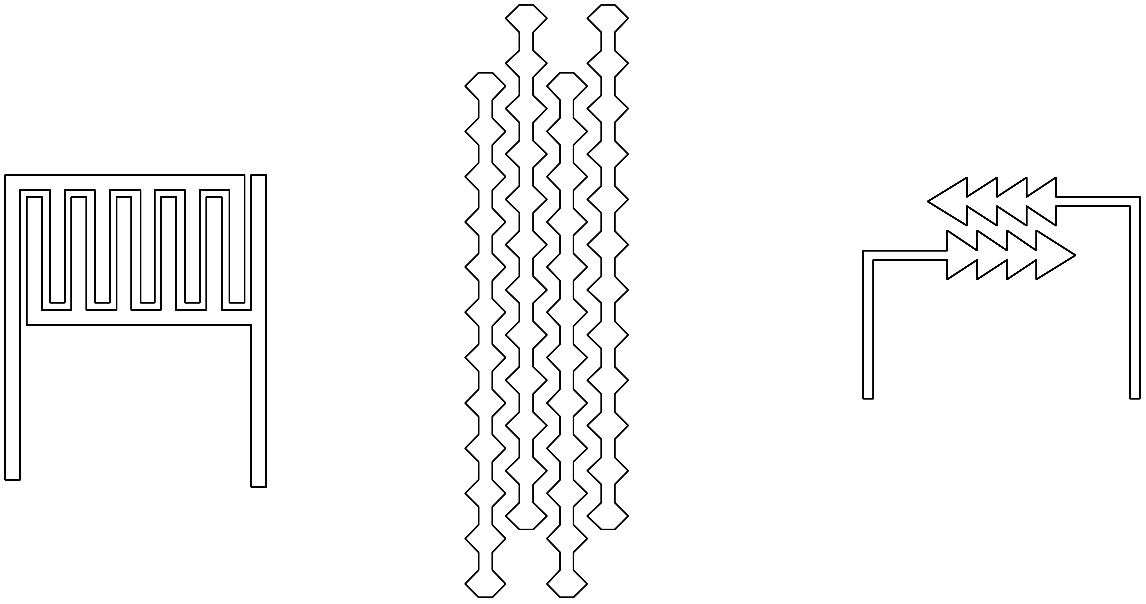

(a) (b) (c)

Figure 3.1 Design of electrode (a) Interdigitated electrodes (b) Saw tooth electrodes (c) Ratchet shaped electrodes

Electrode geometries which were explored are interdigitated, saw tooth and ratchet shaped, respectively. The dimension parameters for the respective electrodes were the width of the electrode and the distance or spacing between them. In the first phase of dimensional variation, the length was kept constant at 1500μm. Keeping the width of the electrodes as constant, the spacing between them was varied from 100μm to 400μm. Now, keeping the spacing between the electrodes as constant, the width of the electrodes was varied from 100μm to 400μm. The electrodes were tested and it was realized that the spacing between the electrodes was not optimized enough. In the second phase, the electrode configuration was changed. This time the spacing between the electrodes was varied from 60μm to 100μm and we got the expected result.

3.1.3 Fabrication

For the electrode layer, a 3-inch COC (Cyclic olefin copolymer) wafer coated with gold (Au) was used. Gold was deposited on the COC wafer by electron beam evaporation. Gold was chosen as the electrode layer for several reasons. The primary reason was its excellent electrical properties and it is easier to etch gold than platinum. The wafer was then spun with Shipley 1813 positive photoresist and patterned to obtain different electrodes. It was finally etched in gold etch solution [potassium iodide + iodine]. The photoresist was stripped by using acetone, methanol and DI water. The wafer was then blow dried with nitrogen gun. The procedure is shown in figure3.2. Individual devices are obtained by dicing the electrode layer.

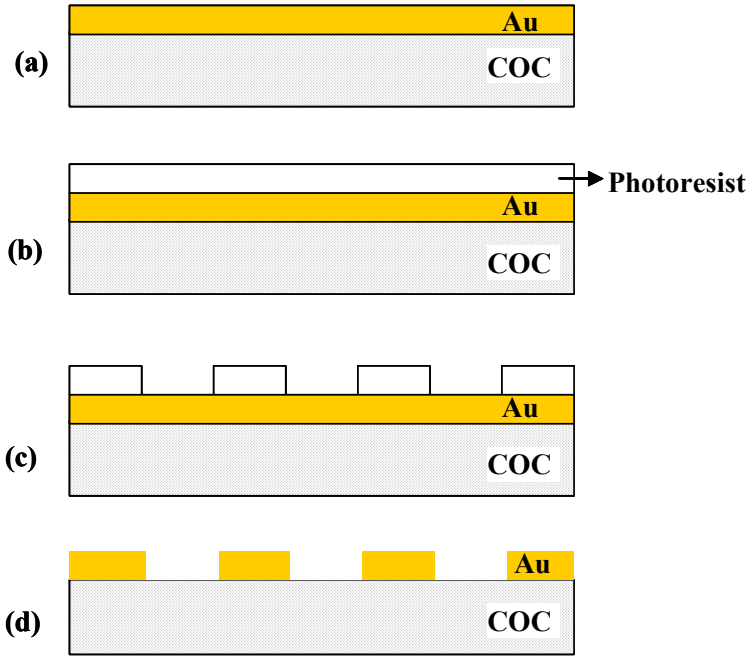

Figure 3.2 Fabrication steps for transferring pattern on a COC wafer (a) Au deposition by evaporation (b) Spin coating of photoresist (c) UV exposure and developing (d) Etching and stripping

3.2 Coulter Counter Electrode

3.2.1 Design

Coulter counter electrode is very simple in design and does not involve the use of any intricate geometrical shapes. It is like a parallel plate capacitor, implying that electrode is usually rectangular in shape. The only variation that can be done is with respect to distance between both the electrodes which are placed across the orifice. Width of each of these rectangular electrodes was 80μm and the gap between them was varied from 1400μm to 1600μm. The microfluidic layer containing the orifice is placed across the electrodes. Two rectangular electrodes are shown in figure 3.3.

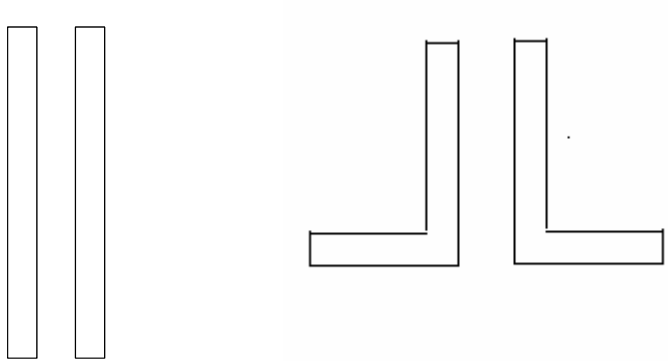

(a) (b)

Figure 3.3 Rectangular electrode shape used for Coulter counter

3.2.2 Fabrication

Electrodes for Coulter counter are fabricated on a COC wafer coated with gold. The fabrication steps for Coulter counter are exactly the same as for dielectrophoresis.

3.3 Fluidic layer

3.3.1 Design

The fluidic layer consists of network of chambers interconnected with each other. All the chambers are either cylindrical or elliptical in shape. These shapes were designed for optimum and smooth flow of the solution. Each microfluidic channel, for Coulter counter consisted of 5 chambers. The dimensions of each channel fabricated using the above-described process were measured. For DEP sensor, the corresponding channel length, channel width and channel depth was 26mm, 1.6mm and 140-145μm respectively. Length of an individual fluidic chamber was 4.4mm. For Coulter counter, each microfluidic channel was 26mm in length, 2mm in width and 140-145μm in height. And each chamber length was 3.9mm in length. For the Coulter counter, the orifice size was varied with respect to its width from 150μm to 250μm.

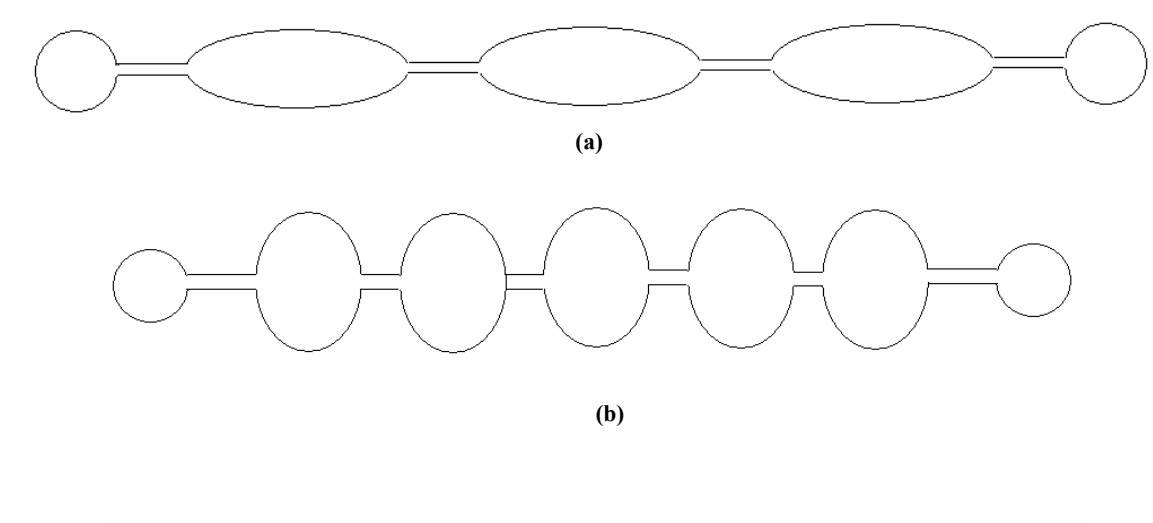

Figure 3.4 (a) Fluidic layer for DEP (b) Fluidic layer for Coulter counter

3.3.2 Fabrication

For the substrate, a 3-inch silicon wafer was used. The wafer was spin coated with adhesion promoter Omnicoat XP before SU-8 2075 (Microchem Corporation XP, Newton, MA) was dispensed and spun onto the wafer which was followed by a one hour time interval that allowed uniform spreading of SU-8. It was then baked at 65^0C for 2 hours and gradually ramped to 95^0C in 30 minutes. The wafer was then cooled to room temperature for atleast 3hours. It was then exposed (2minutes @17.7 mW/cm^2) and baked again at 65^0C for an hour and gradually ramped to 95^0C in 20 minutes. The wafer was allowed to cool down for 2 hours before development. After development, the channel height was confirmed to be 145μm. The structures thus obtained were later used to get microfluidic channels on PDMS.

Thus a negative-tone UV master mold is obtained photolithographically, on a silicon wafer; polydimethylsiloxane (PDMS) elastomer was used to replicate the mold. A curing agent and PDMS prepolymer (SYLGARD 184 Silicone Elastomer Kit, Dow Corning, Midland, MI) were thoroughly mixed in a 1:10 weight ratio. The prepolymer mixture is allowed to relax for 30 minutes so as to remove any air bubbles in the mixture and to insure complete mixing of the two parts. The prepolymer mixture was then poured onto the master in a petridish. It was cured for 12 hours at 65^0C on a hotplate. After curing, the thin PDMS replica was peeled off from the master. The complete procedure is illustrated in the form of a flow chart in figure 3.5. Thereafter, figure 3.6 illustrates the casting process of SU-8 master mold using the PDMS prepolymer.

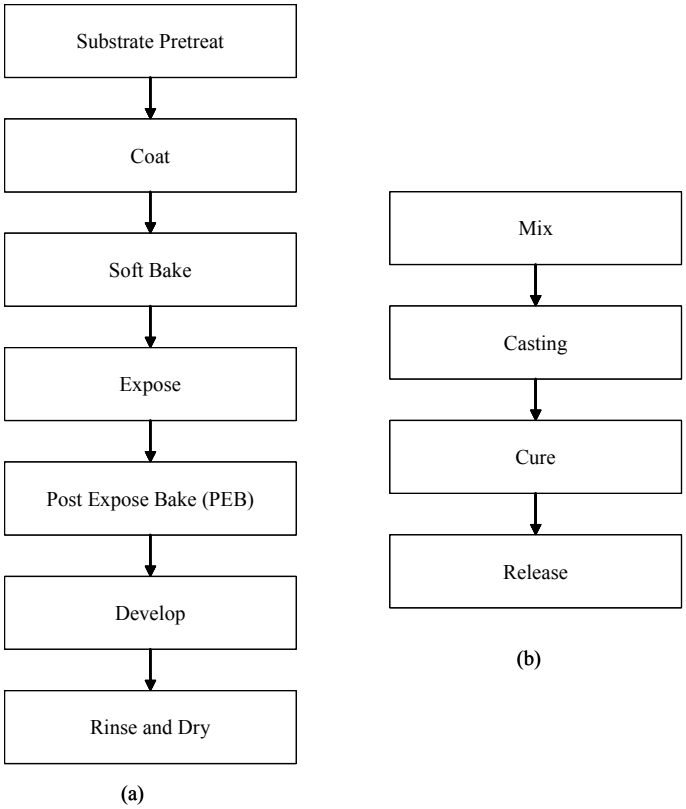

Figure 3.5 Flow chart for the fluidic layer fabrication (a) SU-8 process for a master mold. (b) PDMS replication process for fluidic layer.

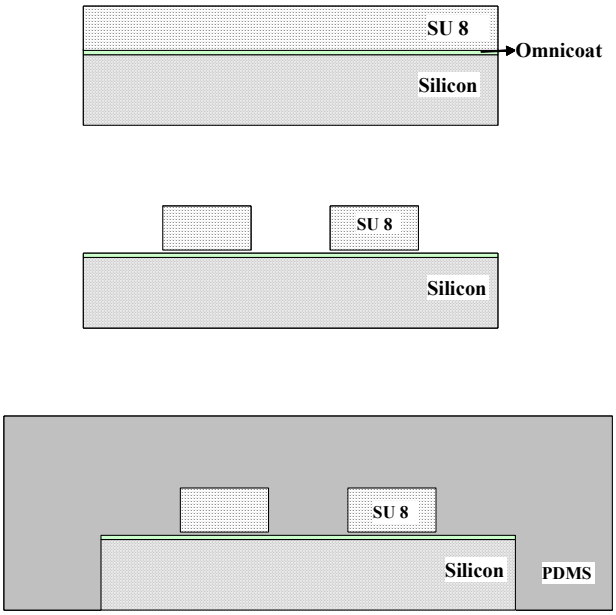

Figure 3.6 Diagrammatical representation of PDMS casting

Figure 3.7 shows the SU-8 microstructures which will be used as the master mold for generating a microfluidic channel using the PDMS polymer.

Figure 3.7 Fabricated structures obtained on a silicon wafer

3.4 Assembly

Figure 3.8 schematically illustrates the electrode layer and the fluidic layers as well as assembled devices. The solution is infused into the chamber through PEEK (polyetheretherketone) tubing which is bonded to holes drilled at the back of COC wafer. For DEP sensor, each fluidic channel has interlinked fluidic chamber which are then properly aligned on top of the electrode with the help of markers.

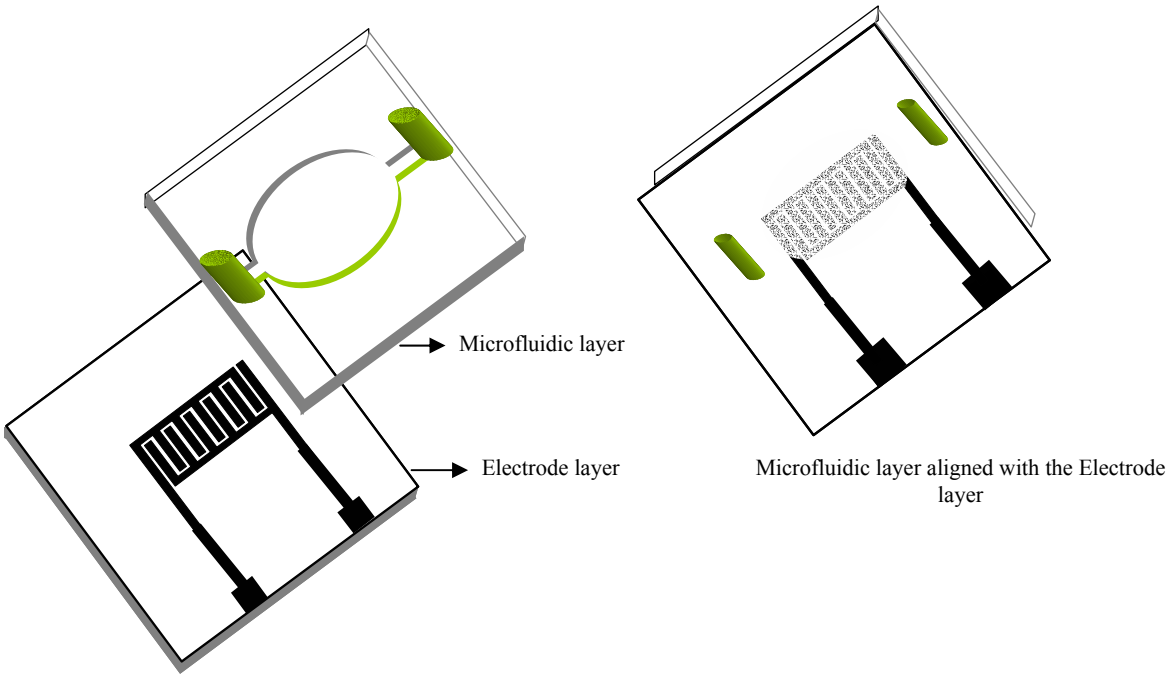

Figure 3.8 (a) before and (b) after assembled view of microfluidic channel and electrode layer

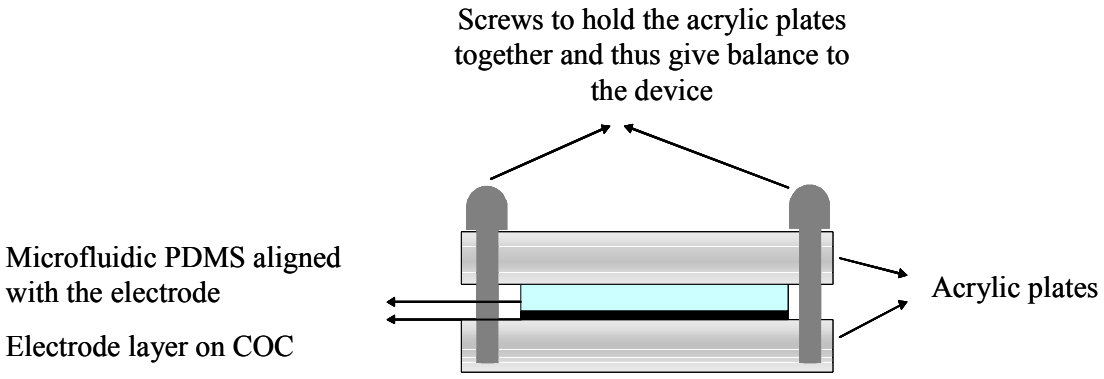

Figure 3.9 An assembled device

In order to provide a robust mechanical support to the wafer section while it was hooked up to all the other various pieces of equipment, a manifold was designed and constructed with the wafer being attached to it as shown in figure 3.9. The manifold was basically a piece of acrylic board with two holes drilled in it. The holes were drilled in such a way, that they corresponded with the inlet and the outlet chamber patterned on the microfluidic layer (PDMS). The wafer section was held in place by sticking it with acrylic in order to ensure minimal movement. Once the entire device had been assembled, the PDMS layer was covered with an acrylic board. The microfluidic layer (top layer) acrylic is screwed together with the bottom layer DEP acrylic. Once the manifold along with the wafer section was in place, integration with other instruments such as the syringe pump, microscope, function generator, and oscilloscope was carried out. Fluidic connections to the device were made by using PEEK (polyetheretherketone) tubing. PEEK tubing is selected over others because it is more robust and bonds well.

CHAPTER 4. CHARACTERIZATION AND RESULTS

4.1 DEP Device Characterization

DEP as an electrokinetic force, depends on applied voltage, radius of the particle suspended in the liquid medium, conductivity of the medium and to some extent on the conductivity of the particle. This work focuses on generating the DEP force and experimentally and mathematically verifying, the dependence of DEP force on the following parameters: applied voltage and conductivity of the medium.

To realize our target, the DEP experiment was carried out in two phases. In both the phases different electrode geometries were used. Conductivity of the medium (and thus complex permittivity of the medium) was varied by using potassium chloride salt. Even though the final application of DEP force is on biological particles, we used polystyrene particles or latex beads as a substitute. In many cases, these beads are used as carriers for bioanalysis. Latex beads of 42μm diameter (Bangs Labs, IN) were used in the experiments. The solution was infused into the device using a programmable syringe pump (NE-100, New Era Pump Systems, NY). a.c. voltage was applied across the contact pads of the electrode geometry to be tested with the help of (Agilent, 33220A, 20MHz Function/Arbitrary Waveform Generator). For observation, digital microscope (Olympus, MIC-D) was used. The images were recorded during experiment. In the first phase, DEP experiment was performed on a saw tooth electrode, as shown in figure 4.2. Applied a.c. signal was varied from 1V to 10V (peak-to-peak). Figure 4.1 shows the experimental setup of the DEP device.

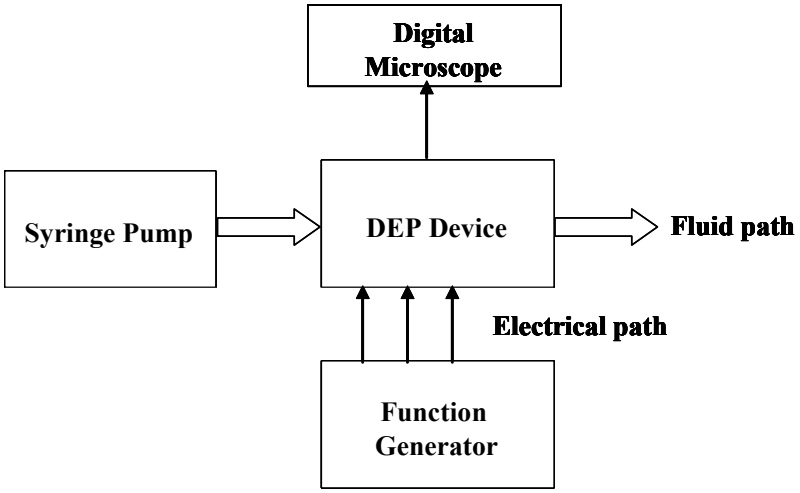

Figure 4.1 Schematic setup for DEP device characterization and testing

Initial experimentation was a common precursor for the two different sets of experiments that followed it. For the first phase characterization, potassium chloride salt was used to make a buffer solution. It was mixed with DI (deionized) water and stirred until the potassium chloride salt was totally dissolved. Its molarity was 0.1M and the conductivity was calculated to be 0.9μS/m. Latex beads of 42μm (diameter) were thoroughly mixed in the conductive solution (5% volume by beads). Conductivity of the latex beads was 10^{-14} μS/m. Permittivity of the medium and bead was calculated to be 22.14* 10^{-12} F/m and 41.1*10^{-12} F/m respectively (equation 3). Using these parameters, Clausius-Mosotti factor, f_{CM} (μS/m) was found out which was .032.

In the second set of experiments, interdigitated electrodes with interelectrode spacing of 80μm were used. From the general DEP force equation (equation 1) it was deduced that the DEP force, besides the electric field gradient, also depends on conductivity of the medium (equation 3). Since, the same kind of particles were experimented upon so the

conductivity of the particle was always constant (σ_p = 10^{-14} μS/m). Therefore, the other parameter that was varied was the conductivity of the medium (σ_m) or Clausius-Mosotti factor. Influence of the medium conductivity variation on the Clausius-Mosotti factor (μS/m) was mathematically analyzed. From this experiment, value of DEP force at different conductivities, for a given applied voltage was found out. Potassium chloride salt was used to make two buffer solutions for our experiment. The molarity and conductivity of one buffer solution were fixed at 0.1M and 0.9 μS/m respectively. For the second set conductivity and molarity were increased to 16μS/m and .11M respectively. The reason for changing the conductivity was to observe variation in other factors. Clausius-Mosotti factor was calculated as 0.222 for the permittivity of $41.1*10^{-12}$ F/m (bead) and $22.14* 10^{-12}$ F/m (medium).

4.2 Coulter Counter Characterization

The orifice of the Coulter counter is the functional part of this device. It is flanked by two simple electrodes for generating the electric field. The position of these electrodes should be close to the orifice for proper functioning of the Coulter counter. The importance of electrode positioning was realized during the initial testing which did not yield any meaningful results. Closer placement of the electrodes to orifice gave us the expected results.

As shown in figure 4.2, other than the regular equipments used for DEP device, two more were needed for the Coulter counter- oscilloscope and high performance digital multimeter. High conductive solution containing suspended latex beads was infused into the device using a syringe pump. The flow rate was monitored and kept constant through out the experiment. A varying a.c. voltage was applied across the contact pads (gold pads) of the Coulter counter. In order to monitor the waveforms generated, a digital oscilloscope

(Tektronix TDS 2012) was used. Change in resistance across the orifice was measured across the multimeter (Agilent 34401A, Multimeter a 6 ½ digit, high performance digital multimeter) in terms of current. Corresponding to change in resistance, variation in the waveform was also observed across the oscilloscope.

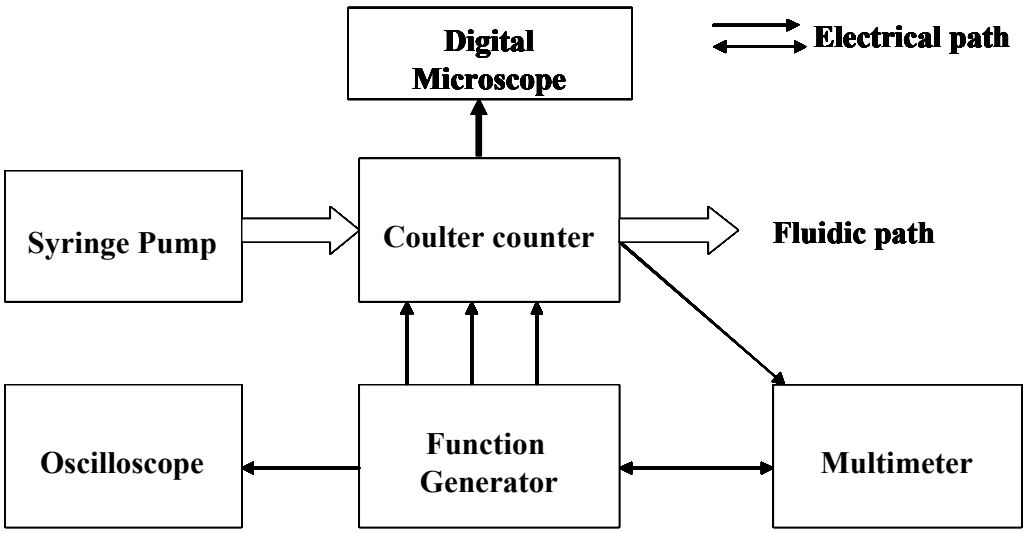

Figure 4.2: Schematic setup for Coulter counter characterization and testing

Polystyrene beads of different diameter were used in this experiment. Diameter of one latex bead was 6.4µm and diameter of the other one was 42µm. Four separate samples were prepared with respect to bead diameter and concentration of the beads suspended in the solution. One was of high concentration (10% volume by beads) and the other was of low concentration (2% beads by volume). Therefore, for high concentration there were two samples 42µm and 6.4µm. By the same logic, for low concentration the two samples were also 42µm and 6.4µm. All the beads were thoroughly mixed in a high conductivity solution. the solution for the experiment was obtained out of 0.19M buffer stock. Conductivity of the medium was 23.3mS/cm.

4.3 Results of DEP Experiments

Saw tooth electrode was selected over other electrodes as most of the DEP experiments used interdigitated ones. So, this was done in order to prove that saw tooth electrodes are as effective as interdigitated ones. For constant f_{CM} (implying constant medium conductivity and constant particle conductivity), the DEP force is calculated with varying distance from the center of inter-electrode spacing. The DEP force value was in the scale of pN, which confirms with the regular DEP force consistent with previous results [15]. Thereby, saw tooth electrode exhibits DEP phenomenon and confirms the viability of this structure. A detailed mathematical analysis on DEP force with varying applied voltage was done using MathCAD software. As illustrated in figure 4.3 with f_{CM} as constant, the DEP force increases with decreasing inter-electrode gap. This fact was conformed by previous results obtained for interdigitated electrodes [13].

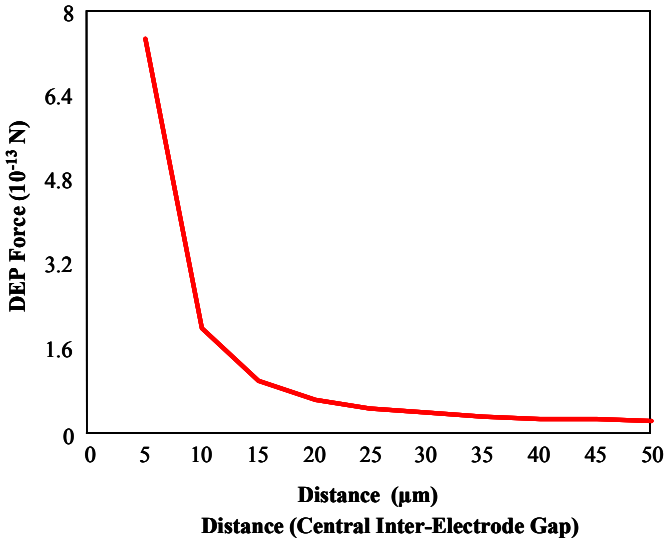

Figure 4.3 Variation in DEP force vs. distance from the centre of inter-electrode spacing

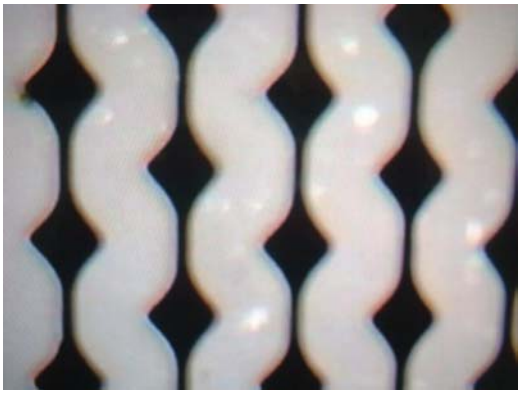

(a)

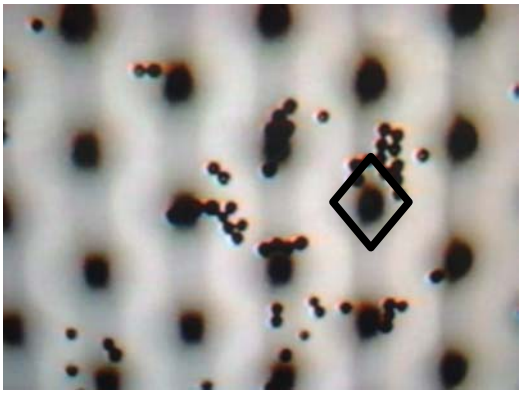

(b)

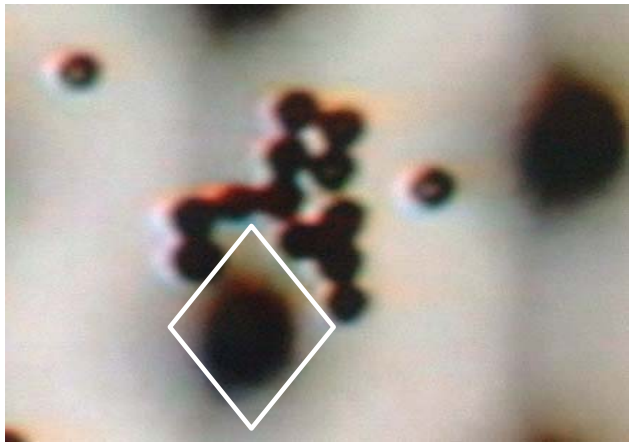

(c)

Figure 4.4 Actual view of DEP experiment (a) Before introducing the sample bead solution (b) Sample under the influence of DEP force (c) Delineated view indicating max DEP force on the edges

As shown in figure 4.4, it was observed that the beads tend to move towards the edges of the saw tooth electrode, and try to cling there, if all other factors are kept constant. This observation validates the fact that electric field is maximum at the edges of an electrode. As we gradually move away from the edge, DEP force rapidly declines and this leads to random movement of the beads. When the flow rate was increased the beads tended to move away

from the electrodes. This implies that the DEP force at that moment was not strong enough to overcome the fluid flow rate.

It is a known fact that variation in conductivity of the medium affects Clausius-Mosotti factor and thus the DEP force. This was verified mathematically and experimentally. As observed, varying the conductivity of the medium gave us different DEP force, for a given voltage. For example, at 5 volts (applied voltage), for conductivity $\sigma_m = 0.9\mu S/m$ the DEP force is around $1.1*10^{-15}N$ or 1.1fN. For the same voltage, at a higher conductivity, $\sigma_m = 16\mu S/m$ the DEP force is around $1.4*10^{-16}N$ or .14fN. This mathematical analysis was confirmed experimentally.

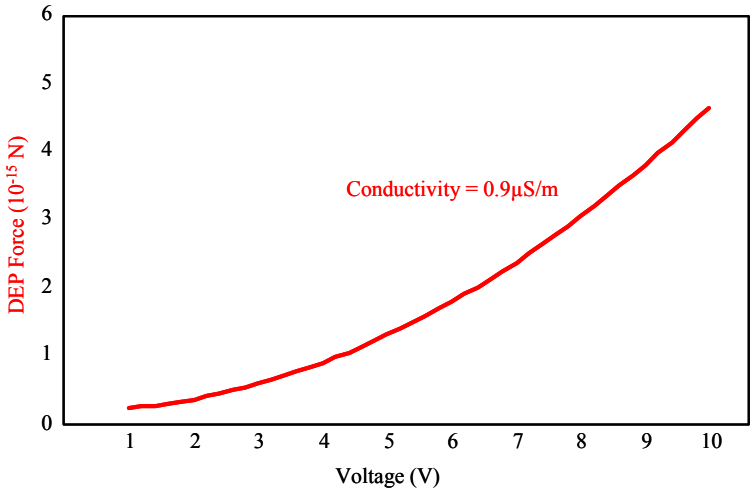

(a)

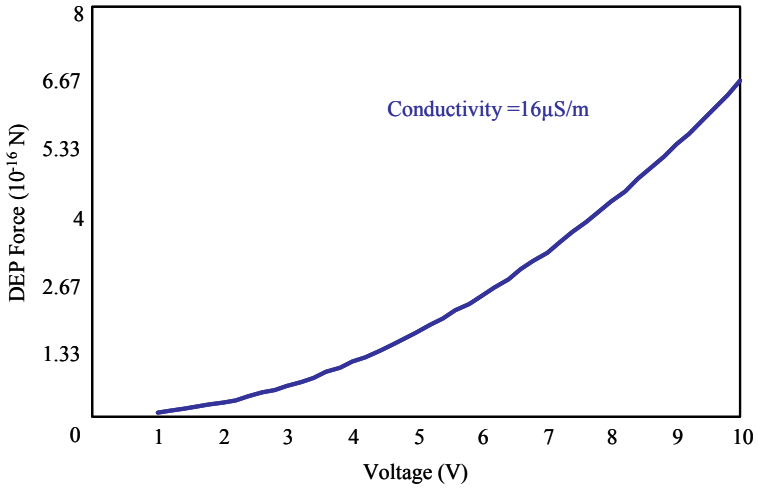

(b)

Figure 4.5 Applied voltage vs DEP force (a) Conductivity = 0.9μS/m
(b) Conductivity = 16μS/m

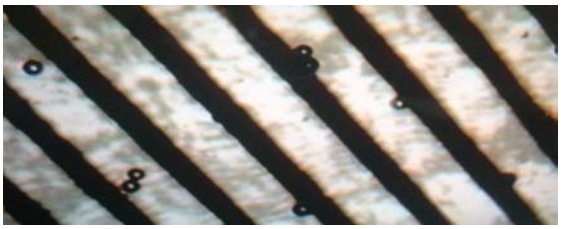

Figure 4.6 Stronger DEP for lower conductivity of the solution, Conductivity = .9μS/m

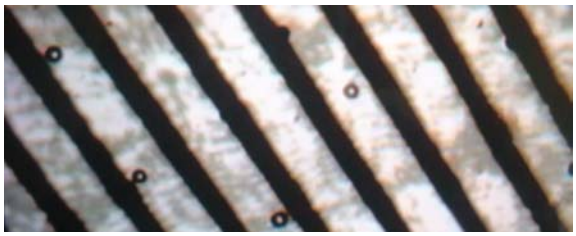

Figure 4.7 Weaker DEP for higher conductivity of the solution, Conductivity = 16μS/m

From figures 4.6 and 4.7, it was clearly visible that for lower conductivity, the DEP force was more because for same flow rate, the applied voltage was less for lower conductivity (to overcome the flow rate and stop the particle from moving) and vice-versa.

By comparing the graph of figure 4.5 with figures 4.6 and 4.7, we can see in the picture that corrsponding to lesser conductivity DEP force is more and thus more particles are collected at the electrode edges.

Figure 4.8 shows the motion of beads as they cross the array of interdigitated electrodes under the influence of applied electric field. Beads were injected alongwith the liquid at a known rate. It was observed that the movement of beads were slow, relative to the transporting medium. Liquid flow rate was calculated to be 4416µm/sec while the rate at which the beads were moving was found to be 1194µm/sec. Hence, it can be inferred that the DEP force was responsible for relatively slow motion of the beads in the liquid.

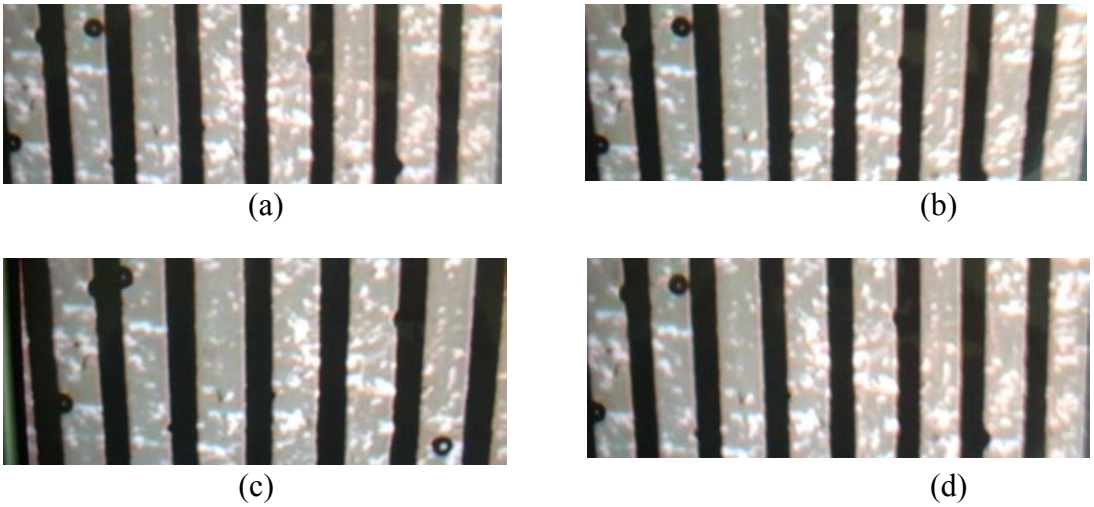

Figure 4.8 (a) (b) (c) (d) Slowed-down movement of latex beads in inter-digitated electrode is shown. Time between each frame is 0.1sec.

4.4 Results of Coulter Counter Experiments

The presupposition for the Coulter principle is a proportionality of the electrical output signal to the particle volume which is experimentally verified. It is evident that as each sample is tested there is a variation in current implying that beads are passing through the orifice thereby causing change in resistance which is measured across the multimeter. For change in current (actually resistance), a corresponding spike is observed across the oscilloscope. This further verified that the device was a Coulter counter prototype, implying that by counting the number of spikes observed across the oscilloscope number of particles can be counted. Therefore, ideally if 5 spikes were observed across the oscilloscope then that means 5 particles had passed through the orifice and thus 5 particles had passed from one chamber to another. But in practical scenario, since the orifice width was 150µm and length of the orifice was 250µm so for 42µm beads three beads can go into the orifice simultaneously. Otherwise, four to five beads can be inside the orifice at the same time. This is known as co-incidence error.

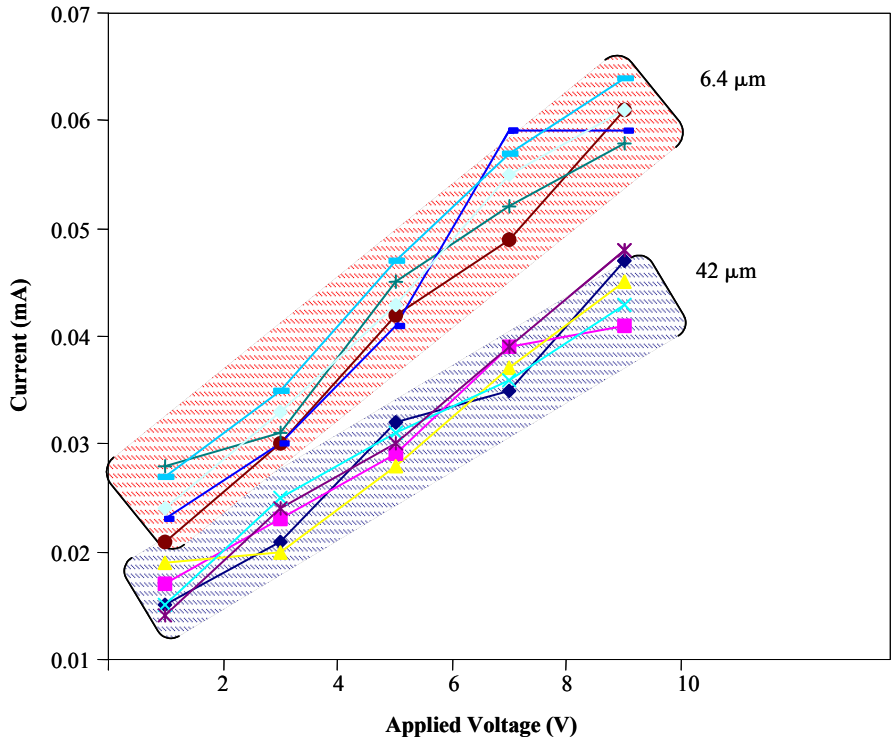

Figure 4.9 For a given conductivity, I-V characteristics of 6.4µm beads and 42µm beads for 2 % beads by volume

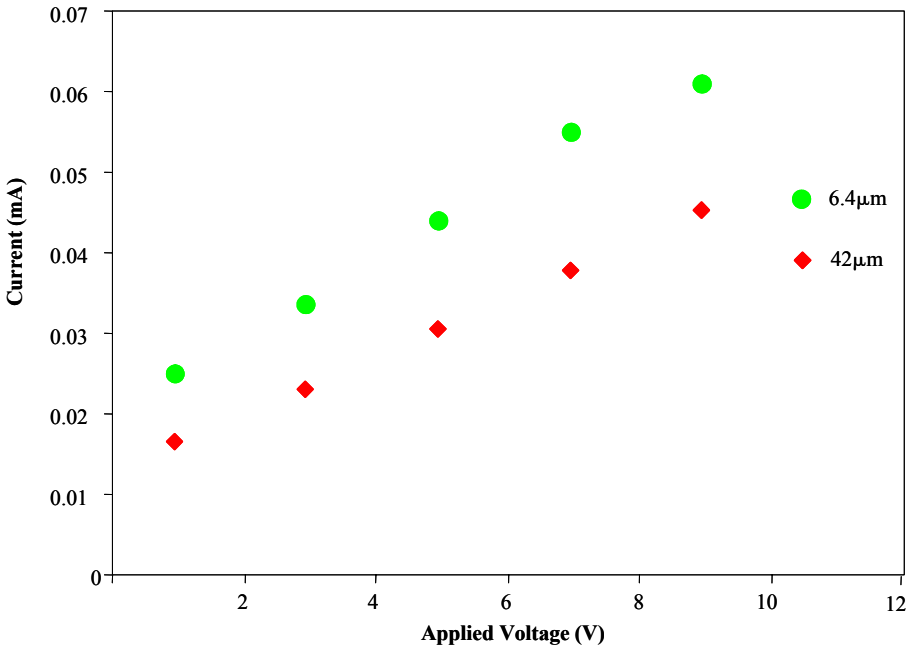

Figure 4.10 Current vs voltage comparison between 6.4µm beads & 42µm beads for 2% beads by volume

Increase in diameter of a bead passing through the Coulter counter orifice causes more displacement of solution causing more resistance in the orifice or less current. This analysis is experimentally verified from figure 4.9 and figure 4.10, because as the diameter of the bead is increased from 6.4µm to 42µ there's an evident fall in current for the same applied voltage.

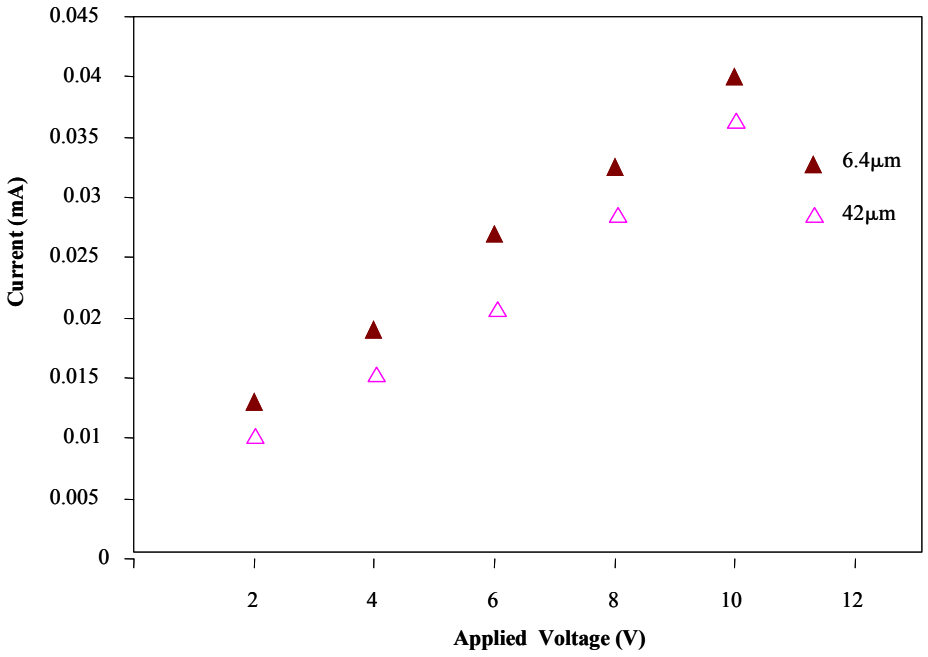

Figure 4.11 Current vs voltage comparison between 6.4µm beads and 42µm beads for 10% beads by volume

When the concentration of the bead in the solution was increased the current for the same bead diameter (for e.g. 42µm) was slightly lesser than one for the lower concentration of beads (for e.g. 42µm) as shown in figure 4.11. This observation is in agreement with the analytical model because at higher concentration more number of beads was in the orifice channel, leading to higher resistance and lower current. Also, the beads may also clump

together and increase the resistance. Another inference is that there is not much change in Coulter counter counting ability with increase in the concentration of beads. Figure 4.12 illustrates the movement of bead in continuous frames, passing through the orifice. Once the bead passes through the orifice an electrical signal is detected by the microelectrode over which the bead solution is passing by.

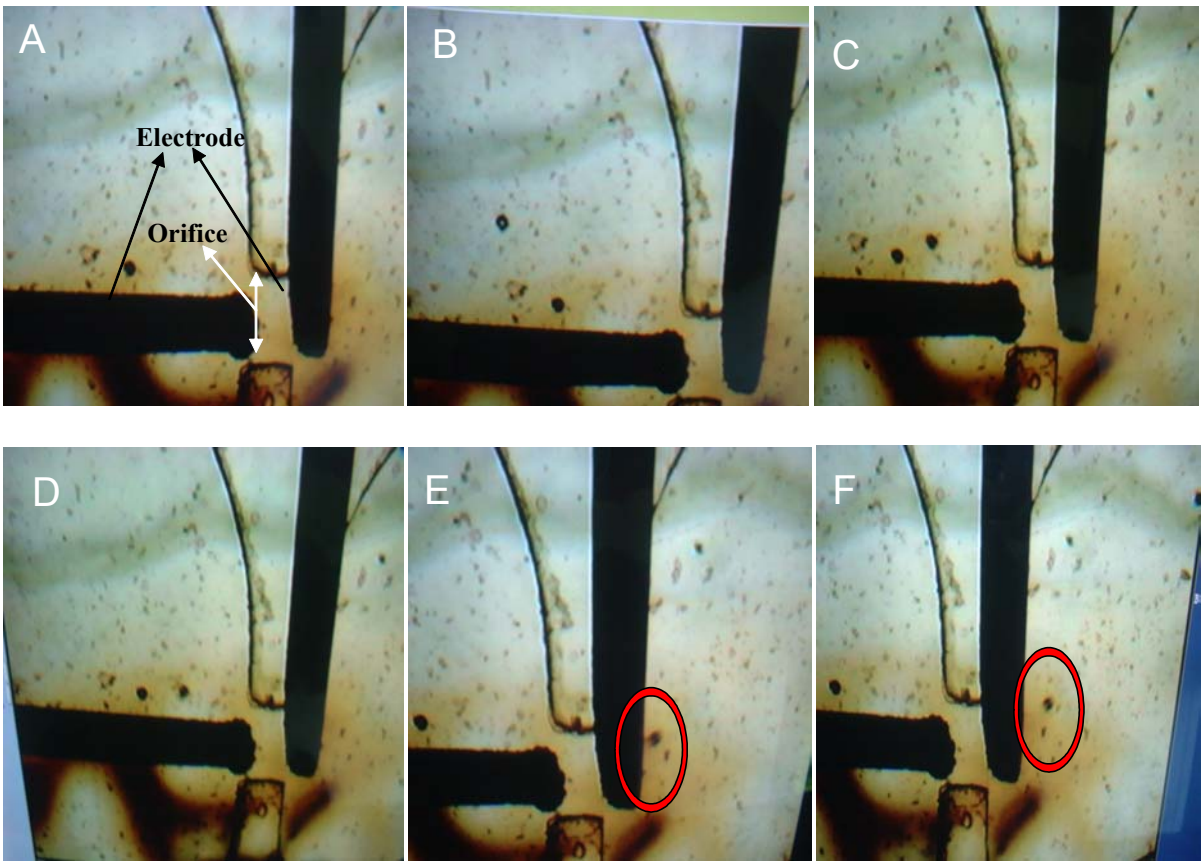

Figure 4.12 Sequential movement of bead passing through (A to F) in a Coulter counter

CHAPTER 5. CONCLUSION AND FUTURE WORK

5.1 Conclusion

In this work dielectrophoresis was studied based on different electrode geometries, applied voltage, and conductivity of the medium. The DEP manipulator was designed, fabricated and characterized. Dielectrophoretic force was mathematically analyzed and showed its ranges from fN to pN. A special case study was done on saw tooth electrodes. Experimentally it was proved that saw tooth electrode exhibits dielectrophoretic force extensively and is as viable as the most widely used interdigitated electrodes. Experimentally and mathematically, the variation of applied voltage and conductivity of the medium with respect to DEP force was analyzed. Miniaturized electrode arrays were fabricated on cyclic olefin copolymer. The fluidic layer was designed separately to include the fluidic channel and interconnections. The fluidic channel was fabricated by using SU-8 used as a master mold and PDMS as the casting material. The Coulter counter was studied for a possible integration of bead counting. Effects of bead size and concentration were studied. The importance of conductivity in both DEP and Coulter counter was verified experimentally.

5.2 Future Work

DEP device developed in this work can be used for separation of same type of particles from a solution and the same can also be used for separating different types of particles by doing more experimental studies. The Coulter counter was developed for counting of beads suspended in a solution. In our studies, oscilloscope (or visual observation)

was used for counting beads. If it is integrated with high speed logic circuits then the bead count can be done automatically. Finally, we will attempt to integrate both separator and a counter, on a chip. Such a device would have widespread implications in clinical biology, combinatorial chemistry and genomics. Experiments are under way by integrating both DEP device and Coulter counter but more studies need to be undertaken especially on their conductivities.

REFERENCES

[1] N.Catsimpoolas, Ed., Methods of Cell Separation, New York: Plenum, 1977.

[2] "Separation and purification: Critical needs and opportunities," National Academy of Sciences – Nat. Res. Council, Washington DC, Report of the Committee of Separation Science and Technology, 1987.

[3] Shapiro, H.M., Practical Flow Cytometry, New York: Alan R. Liss, 1988.

[4] S.Chu, "Laser manipulation of atoms and particles," Science, Vol 253, pp. 861-866, 1991.

[5] T.Lea, J.P. O'Connell, K.Nustad, S.Fusterud, A.Berge and A. Rembaum, " Microspheres as immunoreagents for cell identification and cell fractionation," in Flow Cytometry and Sorting, M.R.Melamed, T.Lidmo, and M.L. Medelsohn, Eds. New York: Wiley-Liss, 1990.

[6] Anne Y. Fu, Charles Spence, Axel Scherer, Frances H. Arnold, and Stephen R.Quake "A microfabricated fluorescence-activated cell sorter", Nature Biotechnology Vol. 17, pp. 1109-1111, 1999.

[7] Janko Auerswald, Helmut F. Knapp "Quantitative assessment of dielectrophoresis as a micro fluidic retention and separation for beads and human blood erythrocytes", Microelectronic Engineering, 67-68, pp. 879-886, 2003.

[8] Giovanni De Gasperis, Jun Yang, Frederick F. Becker, Peter R.C. Gascoyne, and Xiao-Bo Wang "Microfluidic Cell Separation by 2-dimensional Dielectrophoresis", Biomedical Microdevices, 2(1): 41-49, 1999.

[9] Pohl, H.A., Dielectrophoresis, Cambridge University Press, Cambridge, 1978.

[10] P. Marszalek, J.J. Zielinski, and M.Fikus, "Experimental verification of a theoretical treatment of the mechanism of dielectrophoresis," Biochem. Bioenerg.,Vol.22, pp.289-298, 1989.

[11] Y. Huang and R.Pethig, "Electrode design for negative dielectrophoresis", Meas. Sci. Technol., Vol 2, pp. 1142-1146, 1991.

[12] I. Turcu and C. M. Lucaciu, "Dielectrophoresis: a spherical shell mode", J. Phys. A: Math. Gen., 22, No 8, pp.985-993, April 1989.

[13] Xujing Wang, Xiao-Bo Wang, F. F. Becker and Peter R. C. Gascoyne, "A theoretical method of electrical field analysis for dielectrophoretic electrode arrays using Green's theorem", J. Phys. D: Appl. Phys. ,29, No 6, pp.1649-1660, June 1996.

[14] Michael P. Hughes and Hywel Morgan, "An evanescent-field technique for dielectrophoresis studies of colloidal particles", Meas. Sci. Technol.10 No. 8, pp. 759-762, August 1999.

[15] Hywel Morgan, Alberto García Izquierdo, David Bakewell, Nicolas G. Green and Antonio Ramos, "The dielectrophoretic and travelling wave forces generated by interdigitated electrode arrays: analytical solution using Fourier series", J. Phys. D: Appl. Phys., 34, No 10, pp. 1553-1561, May 2001.

[16] M. Koch, A. G. R. Evans and A. Brunnschweiler, "Design and fabrication of a micromachined Coulter counter" J. Micromech. Microeng., 9, No 2, pp. 159-161, June 1999.

[17] S. K. Sikdar and S. H. Webster, "Coulter particle counting at higher counting rates", J. Phys. E: Sci. Instrum. , 13, No 10, pp.1075-1077, October 1980.

[18] Susan Barnes, D. C-H Cheng and H. R. Yarde, “The analysis of Coulter counter data”, Br. J. Appl. Phys., 17, No 11, pp.1501-1506, November 1966.

[19] H. R. Yarde, “An improved method for suspending particles in Coulter counter analyses”, J. Sci. Instrum. , 42, No 9, pp.711-711, September 1965.

[20] Janet Brotherton, “Comparison of the particle size distribution curves determined manually and automatically in an accurately calibrated Coulter counter”, Phys. Med. Biol., 21, No 2, pp.280-284, March 1976.

[21] Francis E. H. Tay, J A van Kan, F Watt and W. O. Choong, “A novel micro-machining method for the fabrication of thick-film SU-8 embedded micro-channels” *J.Micromech. Microeng* 11, 27-32, 2001.

[22] Guerin L. J, Bossel M, Demierre M, Calmes S and Renaud Ph, “Simple and low cost fabrication of embedded micro-channels by using a new thick-film photoplastic” Transducers ’97, pp. 1419-21, June 1997.

[23] P. Renaud, H. Van Lintel, M. Heuschkel, and L. Guerin, “Photo-polymermicrochannel technologies and applications,” in Process. μTAS'98, Banff, Canada, pp. 17–21, October 1998.

[24] B. D. DeBusschere, D. A. Borkholder, and G. T. A. Kovacs, “Design of an integrated silicon-PDMS cell cartridge,” in Solid State Sens. Actuators Conf., Hilton Head, SC, pp. 358–362, June1998.

[25] D. Jaeggi, B. L. Gray, N. J. Mourlas, B. P. Van Drieenhuizen, K. R. Williams, N. I. Maluf, and G. T. A. Kovacs, “Novel interconnection technologies for integrated microfluidic systems,” in Solid State Sens. Actuators Conf., Hilton Head, SC, pp. 112–115, June 1998.

[26] Gravesen P, Branebjerg J and Søndergård Jensen, "Microfluidics-a review", J. Micromech. Microeng. , 3 ,168–82, 1993.

[27] Takayama, S.; McDonald, J. C.; Ostuni, E.; Liang, M. N.; Kenis, P. J. A.; Ismagilov, R. F.; Whitesides, G. M., Proc. Natl. Acad. Sci., 96, 5545-5548, 1999.

[28] Xia Y. N. and Whitesides G. M., "Soft lithography", Angew. Chem. Int. Ed. Engl., 37,551–75, 1998.

[29] Che-Hsin Lin, Gwo-Bin Lee, Bao-Wen Chang and Guan-Liang Chang, "A new fabrication process for ultra-thick microfluidic microstructures utilizing SU-8 photoresist", *J.Micromech. Microeng*., 12, 590-597, 2002.

[30] Eyre B, Blosiu J and Wilberg D., "Taguchi optimization for the processing of EPON SU-8 resist", Proc. MEMS '98 (IEEE, Heidelberg, Germany) pp. 218-22, 1998.

[31] Lorentz H, Despont M, Fahrni N, LaBlance N, Renaud P and Vettiger P., "SU-8: a low cost negative resist for MEMS", *J.Micromech. Microeng.* , **7 ,**121, 1997.

[32] Lorenz H, Despont M, Fahrni M, Brugger J, Vettiger P and Renaud P., "High-aspect-ratio, ultrathick, negative-tone near-UV PR and its applications for MEMS", *Sensors Actuators* A ,64, pp. 33–9,1998.

[33] Zhang J, Tan K. L. and Gong H. Q., "Characterization of the polymerization of SU-8 PR and its applications in micro-electro-mechanical systems (MEMS)" *Polym. Test.,* 20, pp.693–701,2001.

[34] Bogdanov A. L and Peredkov S. S., "Use of SU-8 PR for very high aspect ratio x-ray lithography", *Microelectron. Eng.,* 53, 493–6,2000.

[35] Sampath S. K, Clair L St, Wu X. T, Ivanov D. V, Wang Q, Ghosh C and Farmer K. R., "Rapid MEMS prototyping using SU-8, wafer bonding and deep reactive ion

etching", *Proc. 14th Biennial University/Government/Industry Microelectronics Symp. (IEEE)* pp. 158–61, 2001.

[36] Ewan H. Conradie and David F. Moore, "SU-8 thick photoresist processing as a functional material for MEMS applications", *J.Micromech. Microeng.,* 12, 368-374, 2002.

[37] Francis E. H. Tay, J A van Kan, F Watt and W. O. Choong, "A novel micro-machining method for the fabrication of thick-film SU-8 embedded micro-channels", *J.Micromech. Microeng* ,11, pp.27-32, 2001.

[38] Guerin L. J, Bossel M, Demierre M, Calmes S and Renaud Ph, "Simple and low cost fabrication of embedded micro-channels by using a new thick-film photoplastic", Transducers '97, pp. 1419-21, 1997.

[39] Duffy D. C, McDonald J C, Schueller, O. J. A and Whitesides G. M., "Rapid prototyping of microfluidic systems in poly(dimethylsiloxane)", Anal. Chem. 70 pp.4974-84, 1998.

[40] Chen X X, Wu H K, Mao C D and Whitesides G. M. , "A prototype two-dimensional capillary electrophoresis system fabricated in poly(dimethylsiloxane)", Anal. Chem., 74, pp.1772–8, 2002.

[41] Yang T, Jung S. Y, Mao H and Cremer P. S, "Fabrication of phospholipid bilayer coated microchannels for immunoassays", Anal. Chem., 73, pp.165–9, 2001.

[42] Anderson J. R, Chiu D. T, Jackman R J, Cherniavskaya O, McDonald J. C, Wu H, Whitesides S. H and Whitesides G. M, "Fabrication of topologically complex three-dimensional microfluidic systems in PDMS by rapid prototyping", Anal.Chem.,72, pp.3158–64, 2000.

[43] http://www.alcanpackaging.com/cosmetics/eng/html/resins.php